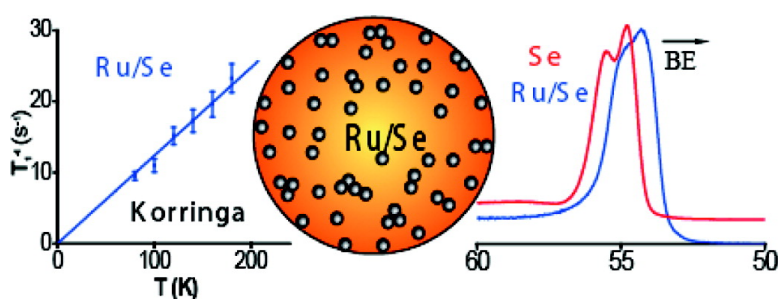


## Selenium Becomes Metallic in Ru–Se Fuel Cell Catalysts: An EC-NMR and XPS Investigation

Panakkattu K. Babu, Adam Lewera, Jong Ho Chung, Ralf Hunger, Wolfram Jaegermann, Nicolas Alonso-Vante, Andrzej Wieckowski, and Eric Oldfield

*J. Am. Chem. Soc.*, **2007**, 129 (49), 15140-15141 • DOI: 10.1021/ja077498q

Downloaded from <http://pubs.acs.org> on February 9, 2009



### More About This Article

Additional resources and features associated with this article are available within the HTML version:

- Supporting Information
- Access to high resolution figures
- Links to articles and content related to this article
- Copyright permission to reproduce figures and/or text from this article

[View the Full Text HTML](#)

## Selenium Becomes Metallic in Ru–Se Fuel Cell Catalysts: An EC-NMR and XPS Investigation

Panakkattu K. Babu,<sup>§</sup> Adam Lewera,<sup>†</sup> Jong Ho Chung,<sup>§</sup> Ralf Hunger,<sup>‡</sup> Wolfram Jaegermann,<sup>‡</sup> Nicolas Alonso-Vante,<sup>‡</sup> Andrzej Wieckowski,<sup>\*,§</sup> and Eric Oldfield<sup>\*,§</sup>

Department of Chemistry, University of Illinois at Urbana-Champaign, Urbana, Illinois, Department of Chemistry, Warsaw University, Warsaw, Poland, Institute of Materials Science, University of Technology, Darmstadt University, Darmstadt, Germany, and Laboratory of Electrocatalysis, University of Poitiers, France

Received September 28, 2007; E-mail: andrzej@scs.uiuc.edu; eo@chad.scs.uiuc.edu

The large-scale commercialization of fuel cells depends on the optimal choice of fuel as well as on the development of cost-effective electrocatalysts.<sup>1</sup> When using hydrogen as a fuel, issues related to hydrogen production and storage pose serious challenges. Alcohol fuel cells are one possible alternative to hydrogen fuel cells; however, traditional platinum-based fuel cell cathodes suffer from unfavorable overpotentials for the oxygen reduction reaction (ORR), poor methanol tolerance, and the high cost of platinum. The development of novel, platinum-free cathode catalysts with high methanol tolerance is, therefore, an important goal of broad general interest and significance.

One approach to the development of more cost-effective cathode materials for the ORR is the use of clusterlike chalcogenides, which have the great advantage of being selective for oxygen reduction in the presence of methanol. For example, in recent work we developed a new binary cathode catalyst, Ru/Se, through surface modification of Ru nanoparticles<sup>2</sup> and showed that this catalyst was more efficient than Pt, in methanol containing acidic media. However, while the importance of chalcogen additives in the ORR activity and stability of Ru has been recognized in clusterlike chalcogenides<sup>3</sup> and in surface modified Ru nanoparticle catalysts,<sup>2</sup> little is known about how the electronic properties of Ru are modified due to the addition of Se. Here, we use electrochemical nuclear magnetic resonance (EC-NMR) and X-ray photoelectron spectroscopy (XPS) to investigate this question. Our results show for the first time that Se, a p-type semiconductor in elemental form, becomes metallic when interacting with Ru in Ru–Se catalysts, due to charge transfer from Ru to Se. Ru surfaces modified in this way show exceptional chemical stability in acidic media, even at high positive potentials.

Ru–Se chalcogenide catalysts were synthesized as described previously,<sup>2,3</sup> and details of the EC-NMR and XPS measurements are given in the Supporting Information. We first investigated the <sup>77</sup>Se NMR spectra of the two catalyst samples, Ru/Se (with a ruthenium to selenium ratio, Ru:Se = 3.3:1) and Ru<sub>x</sub>Se<sub>y</sub> (Ru:Se ≈ 2:1), both of which showed very high activity in the ORR. As can be seen in Figure 1a, the <sup>77</sup>Se NMR spectra of both samples at 80 K exhibit similar shifts,  $\delta \approx 1670$  ppm (from aqueous H<sub>2</sub>SeO<sub>3</sub>). The overall line width of the Ru/Se sample is greater than that of Ru<sub>x</sub>Se<sub>y</sub>, because to the larger heterogeneity of the Ru surface sites in the catalyst prepared from commercial Ru nanoparticles. In contrast, the <sup>77</sup>Se NMR spectrum of elemental Se is far narrower, Figure 1a, with three partially resolved peaks, corresponding to the three nonequivalent Se sites seen crystallographically.<sup>4</sup> The center

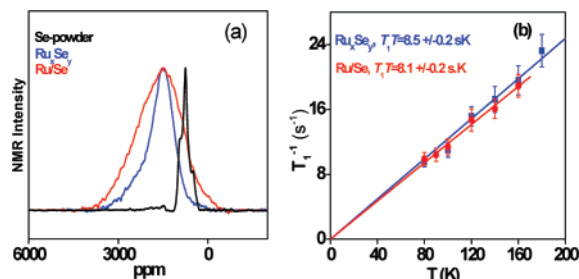


**Figure 1.** (a) <sup>77</sup>Se NMR spectra of Se powder, Ru/Se, and Ru<sub>x</sub>Se<sub>y</sub> catalysts obtained at 8.45 T and 80 K. (b) Temperature dependence of the spin–lattice relaxation rate in the two catalyst samples. Both have very similar  $T_1T$  values.

of mass of the elemental Se NMR spectrum occurs at 857 ppm, so there is a  $\sim 813$  ppm downfield shift for Se atoms when bonded to Ru.

While the large downfield shift from Se  $\rightarrow$  Ru–Se could in principle contain a substantial orbital or chemical-shift contribution, it is also possible that the observed shift could contain a large Knight shift contribution, in which case a large effect on the spin–lattice relaxation time ( $T_1$ ) would be expected, due to strong interactions between conduction electrons and the <sup>77</sup>Se nuclei.<sup>5</sup> This is found to be the case. In particular, we found the  $T_1$  value for <sup>77</sup>Se in elemental Se powder to be  $\sim 400$  s at 80 K, while the  $T_1$  values for both Ru/Se and Ru<sub>x</sub>Se<sub>y</sub> were only  $\sim 100$  ms (at 80 K). In addition to this 3 orders of magnitude reduction in  $T_1$ , the catalyst samples also show very different behavior with respect to the temperature dependence of  $T_1$ . For elemental Se,  $T_1$  follows a  $T^2$  dependence, characteristic of the 2-phonon relaxation mechanism seen with other electrically insulating materials, since the band gap for Se (1.8 eV) is so large that the concentration of intrinsic conduction electrons is negligible.<sup>6</sup> However, with both the Ru/Se and Ru<sub>x</sub>Se<sub>y</sub> catalyst samples, we find the purely Korringa behavior characteristic of metals, in which  $1/T_1 \propto T$ . The temperature dependence of the spin–lattice relaxation rate ( $T_1^{-1}$ ) is shown in Figure 1b, and from the slopes we deduce Korringa constants ( $T_1T$ ) of  $8.1 \pm 0.2$  s·K for Ru/Se and  $8.5 \pm 0.2$  s·K for Ru<sub>x</sub>Se<sub>y</sub>.

The Korringa behavior arises because of hyperfine interactions between the <sup>77</sup>Se nuclei and the conduction electrons and is given by<sup>5</sup>

$$T_1TK^2 = \frac{\hbar}{4\pi k_B} \left( \frac{\gamma_e}{\gamma_n} \right)^2 B \quad (1)$$

where  $\gamma_e$  and  $\gamma_n$  are the gyromagnetic ratios of the electron and the nucleus, respectively,  $K$  is the Knight shift, and  $B$  represents a factor equal to unity, except when electron–electron interactions are large. Such electron–electron interactions are small for surface

<sup>§</sup> University of Illinois at Urbana-Champaign.

<sup>†</sup> Warsaw University.

<sup>‡</sup> Darmstadt University.

<sup>‡</sup> University of Poitiers.

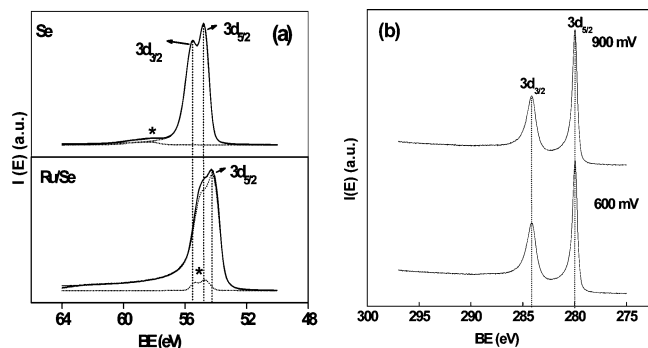


**Figure 2.** (a) XPS spectra of Se powder and the Ru/Se catalyst, in the Se 3d region. The asymmetric line shape seen in the catalyst indicates Se becomes metallic, the shift indicates Ru  $\rightarrow$  Se charge transfer (\*= peaks due to traces of SeO<sub>2</sub> and elemental Se). (b) XPS spectra for the Ru/Se nanoparticle catalyst in the Ru 3d region, polarized to 600 and 900 mV vs RHE in 0.1 M H<sub>2</sub>SO<sub>4</sub>. Because of Ru–Se interactions, there is no Ru oxidation at these high potentials, as there would be for bare Ru. Spectra recorded at 370 eV excitation energy.

species<sup>7</sup> (i.e.,  $B \approx 1$ ), so we can estimate a Knight shift of 929 ppm which is clearly similar to the  $\sim 813$  ppm shift difference between elemental Se and the Ru–Se catalysts seen experimentally, Figure 1a. These shift and spin–lattice relaxation results clearly indicate, therefore, that Se becomes metallic when it binds to Ru, although qualitatively, the Korringa constant is closer to that seen with other adsorbates (e.g., <sup>13</sup>CO,  $T_1T \approx 80$  s·K) than with bulk transition metals (e.g., <sup>195</sup>Pt,  $T_1T \approx 0.03$  s·K), indicating a relatively low Fermi level density of states ( $E_F$ -DOS).

To try to gain further insight into the nature of the Ru–Se interaction, we next investigated the XPS spectra of Ru/Se (and Se) in the 3d<sub>3/2</sub>–3d<sub>5/2</sub> binding energy (BE) region. The XPS spectrum of Ru/Se in the Se 3d region (Figure 2a) shows two important features. First, the main peak in Ru/Se has an asymmetric line shape, characteristic of a metallic system. Second, the main peak (Se 3d<sub>5/2</sub>) is shifted toward lower BE (by  $0.5 \pm 0.02$  eV) compared to that in elemental Se. The XPS line shape in Figure 2a is well described by the Doniach–Šunjić function:<sup>8</sup>

$$Y(E) = \frac{\Gamma(1 - \alpha)}{[(E - E_0)^2 + \gamma^2]^{(1-\alpha)/2}} \cos \times \left[ \frac{\pi\alpha}{2} + (1 - \alpha) \tan^{-1} \left( \frac{E - E_0}{\gamma} \right) \right] \quad (2)$$

where  $Y$  is the intensity,  $\Gamma$  is the gamma function,  $E_0$  is the binding energy,  $\gamma$  is the lifetime broadening of the core level, and  $\alpha$  is the asymmetry parameter. This function reduces to a Lorentzian with full-width at half-maximum height of  $2\gamma$  for  $\alpha = 0$ , and a nonzero  $\alpha$  value indicates a finite  $E_F$ -DOS.<sup>8</sup> In the case of the Ru/Se catalyst sample, the deconvolution shows that the main Se peak (3d<sub>5/2</sub>) has  $\alpha = 0.12 \pm 0.01$ , while the same analysis for Se powder yields  $\alpha = 0.02 \pm 0.01$ . The  $\alpha = 0.12 \pm 0.01$  value for Ru/Se thus indicates a finite  $E_F$ -DOS, that is, metallic behavior, for Se. XPS spectra of semiconductors do not show the Doniach–Šunjić asymmetry in these core-level peaks, because the band gap eliminates the possibility of exciting low-energy electron–hole pairs, so an asymmetric line shape is not seen. These results are, of course, completely consistent with the observation of Korringa-behavior in the <sup>77</sup>Se NMR experiments on the Ru–Se catalyst samples. Moreover, the Se 3d BE shift observed in Ru/Se suggests a likely origin for the semiconductor  $\rightarrow$  metal transition for Se.

Specifically, the negative shift in BE can be attributed to charge transfer from Ru to the far more electronegative Se (Allred–

Rochow electronegativity of 2.48 for Se versus 1.42 for Ru), since this will increase the electron–electron repulsion within the Se atoms, moving the Se core levels toward lower BE.<sup>9</sup> This charge transfer from surface Ru to Se makes Ru less susceptible to oxidation, which we propose as the most likely explanation for the unusual stability of metallic Ru in these systems, even at high electrode potentials. Paradoxically, this charge transfer does not produce any observable core level BE shift for Ru, as can be seen from the XPS spectra (Figure 2b), which are identical to those of elemental Ru.<sup>11</sup> However, consistent with this, earlier studies have shown that the core level BE for Ru does in fact show very little variation with composition in other alloy or surface-modified bimetallic nanoparticle catalysts<sup>10,11</sup> due, it has been proposed, to the open d-shell configuration of Ru.<sup>12</sup>

These results are of interest for the following reasons: First, we report the first <sup>77</sup>Se NMR investigation of Ru–Se ORR fuel cell catalyst. The results clearly prove that Se becomes metallic when bound to Ru, as indicated by the large Knight shift ( $\sim 800$  ppm) and the Korringa relaxation ( $T_1T \approx 8$  s·K), for both types of catalyst. Second, the XPS line shape confirms the metallic nature of Se on Ru/Se, and the BE shift suggests that the Ru  $\rightarrow$  Se charge transfer is responsible for this effect. Third, our results suggest that the enhanced activity of these catalyst samples in the ORR can be attributed to this Ru  $\rightarrow$  Se charge transfer, which renders Ru less susceptible to electron withdrawal, that is, to oxidation, even at high-electrode potentials. These results may facilitate the design of other stable and potent fuel cell electrocatalysts, by combining two or more elements to induce electronic alterations on a major catalytic component, similar to the effects seen on Se addition to Ru.

**Acknowledgment.** This work was supported by the Army Research Office (MURI Grant DAAD19-03-1-0169 for fuel-cell research to Case Western Reserve University), NSF Grant CHE06-51083, and a DOE Grant (LANL 53183-001-7) from Office of Hydrogen, Fuel Cells & Infrastructure Technologies. We thank Patrick Hoffmann and Dieter Schmeißer (BTU Cottbus) in operating the U49/2-PGM2 beam line and Sascha Hümann (University of Bonn) for his valuable contributions to the design, construction, and operation of the electrochemical setup. Partial support (to A.L.) from Warsaw University under Grant BW-175606 and from the Ministry of Science and Higher Education (Poland) (N204 16423/4284) is also appreciated.

**Supporting Information Available:** Experimental details for sample preparation, NMR, and XPS measurements. This material is available free of charge via the Internet at <http://pubs.acs.org>.

## References

- (1) Steele, B. C. H.; Heinzel, A. *Nature* **2001**, *414*, 345–352.
- (2) Cao, D.; Wieckowski, A.; Inukai, J.; Alonso-Vante, N. *J. Electrochem. Soc.* **2006**, *153*, A869–A874.
- (3) Alonso-Vante, N. In *Catalysis of Nanoparticles Surfaces*; Wieckowski, A., Savinova, E., Vayenas, C., Eds.; Marcel Dekker, Inc.: New York, 2003; p 931.
- (4) Koma, A. *Phys. Stat. Solidi B* **1973**, *56*, 655–664.
- (5) Slichter, C. P. *Principles of Magnetic Resonance*, 3rd ed.; Springer-Verlag: 1992.
- (6) Günther, B.; Kanert, O. *Phys. Rev. B* **1985**, *31*, 20–33.
- (7) Rudaz, S. L.; Ansermet, J. P.; Wang, P. K.; Slichter, C. P. *Phys. Rev. Lett.* **1985**, *54*, 71–74.
- (8) Doniach, S.; Šunjić, M. *J. Phys. C* **1970**, *3*, 285–290.
- (9) Egelhoff, W. F. *J. Surf. Sci. Rep.* **1987**, *6*, 253–415.
- (10) Kim, H.; Rabelo de Moraes, I.; Tremiliosi-Filho, G.; Haasch, R.; Wieckowski, A. *Surf. Sci.* **2001**, *474*, L203–212.
- (11) Lewera, A.; Zhou, W. P.; Vericat, C.; Chung, J. H.; Haasch, R.; Wieckowski, A.; Bagus, P. S. *Electrochim. Acta* **2006**, *51*, 3950–3956.
- (12) Lewera, A.; Zhou, W. P.; Hunger, R.; Jaegermann, W.; Wieckowski, A.; Yockel, S.; Bagus, P. S. *Chem. Phys. Lett.* **2007**, *447*, 39–43.

JA077498Q